Agricultural and Forest Meteorology 230–231 (2016) 33–44

Contents lists available at ScienceDirect

Agricultural and Forest Meteorology

journal homepage: www.elsevier.com/locate/agrformet

Evaluating the complementary relationship for estimating evapotranspiration using the multi-site data across north China

Gao-Feng Zhu[a,*], Kun Zhang[a], Xin Li[b,c], Shao-Min Liu[d], Zhen-Yu Ding[e], Jin-Zhu Ma[a], Chun-Lin Huang[b,f], Tuo Han[a], Jian-Hua He[a]

[a] Key Laboratory of Western China's Environmental Systems (Ministry of Education), Lanzhou University, Lanzhou 730000, China
[b] Key Laboratory of Remote Sensing of Gansu Province, Cold and Arid Regions Environmental and Engineering Research Institute, Chinese Academy of Sciences, Lanzhou 730000, China
[c] Chinese Academy of Sciences Center for Excellence in Tibetan Plateau Earth Sciences, Beijing 100101, China
[d] State Key Laboratory of Remote Sensing Science, School of Geography, Beijing Normal University, Beijing 100875, China
[e] Chinese Academy For Environmental Planning, Beijing 100012, China
[f] Jiangsu Center for Collaborative Innovation in Geographical Information Resource Development and Application, Nanjing 210023, China

ARTICLE INFO

Article history:
Received 14 November 2015
Received in revised form 7 April 2016
Accepted 7 June 2016
Available online 20 June 2016

Keywords:
Actual evapotranspiration
Complementary relationship
Granger and gray model
North China
Temporal scales

ABSTRACT

The ability to predict actual evapotranspiration flux (λE_a) by physically based evaporanspiration (ET) model is limited globally due to the difficulty in validating the site-specific model parameters. Thus, the approaches for estimating λE_a using only routine meteorological variables play a critical role in understanding and predicting hydrological cycle in the context of climate change. In this study, the performance of a complementary relationship (CR) method (Granger and Gray, 1989; GG model) on different timescales (daily and half-hourly) was evaluated using a high-quality dataset of selected 12 eddy covariance flux towers, which encompassed a number of cropland, grassland, evergreen needleleaf forest, desert shrub and wetland sites across northern China. The results indicated that the GG model is applicable in estimating daily λE_a for most ecosystems across northern China. However, significant underestimations of daily λE_a were found for the croplands (Daman and Dunhuang sites) and the desert shrub (Ejina) in the arid northwest China, which may be attributed to the enhanced λE_a by horizontal advection and the deep root water-uptake, respectively. By using the Monin-Obukhov similarity theory with a surface energy balance constraint, the model performance on half-hourly timescale was satisfactory for the 12 tower sites with R^2 ranging from 0.54 to 0.81 and the slopes of Deming regression line between measured and simulated λE_a from 0.77 to 1.14. Indeed, the study highlights the need for further investigation of the timescale dependence of the CR-based ET models.

1. Introduction

Evapotranspiration (ET) is an important land surface process in climatology and a nexus for modeling terrestrial water, energy and carbon cycles (Jung et al., 2010). Thus accurate estimation of ET (or λE_a, i.e., latent heat flux, where λ is the latent heat of vaporization) on a daily or subdiurnal time steps is crucial to a wide range of problems in hydrology (Xu and Singh, 2005; Zhu et al., 2013), agronomy (Zhu et al., 2014a), macroecology (Fisher et al., 2011), and weather and climate prediction (Wang and Dickinson, 2012). In this paper, ET or λE_a is used interchangeably depending on whether water or energy flux is the primary consideration. There exist a multitude of one- or two-source physically based models to estimate λE_a (Penman, 1948; Monteith, 1965; Shuttleworth and Wallace, 1985; Lhomme and Chehbouni, 1999). Unfortunately, validating site-specific model parameters such as the aerodynamic, canopy, and soil resistances remains challenging (Salvucci and Gentine, 2013), resulting in their practical use at regional or global scales to be limited (Xu and Singh, 2005). Hence, it is important to find a way to derive λE_a using standard meteorological variables without detailed knowledge of the surface states (e.g., leaf area, soil texture, soil moisture and stomatal conductance) (Brutsaert, 2005; Crago and Crowley, 2005; Salvucci and Gentine, 2013).

* Corresponding author at: 222 South Tianshui Road, Lanzhou City, Gansu Province 730000, China.
E-mail address: zhugf@lzu.edu.cn (G.-F. Zhu).

http://dx.doi.org/10.1016/j.agrformet.2016.06.006
0168-1923/

For this purpose, a complementary relationship (CR) was first proposed by Bouchet (1963) forming the basis for the development of several ET models. These include the complementary relationship areal evapotranspiration (CRAE) model (Morton, 1983) and the advection-aridity (AA) model (Brutsaert and Stricker, 1979). It should be noted that the CR between actual and potential evapotranspiration was constrained to be symmetric in the CRAE and AA models. Despite considerable work, some studies claim that the assumed symmetric nature of the CR may be invalid for certain conditions (Kahler and Brutsaert, 2006; Szilagyi et al., 2009; Pettijohn and Salvucci, 2006, 2009; Crago and Qualls, 2013). Thus, many researchers have attempted to develop rigorous derivations of the CR (Crago and Qualls, 2013). Granger and Gray (1989) first derived an asymmetric CR to estimate λE_a by using a procedure similar to that of Penman (1948) (hereafter referred to GG model). Interestingly, Szilagyi (2007) obtained the same operational ET model as the GG model although through different theoretical considerations of Granger and Gray's (1989). Over the past decades, numerous studies were carried out to either evaluate or compare the performance of the CR-based ET models. For example, Crago and Crowley (2005) illustrated that the GG model performed by far the best among the six CR-based ET models in a comparative study. Also, it has been reported that significant bias (i.e., underestimation of λE_a for dry conditions and overestimation of λE_a for wet conditions) may result in the AA model (Ali and Mawdsley, 1987; Crago and Brutsaert, 1992; Qualls and Gultekin, 1997; Hobbins et al., 2001). However no similar observations were found for the GG model (Han et al., 2011; Xu and Chen, 2005). Recently, Anayah and Kaluarachchi (2014) reported that the GG model was the most attractive when compared to the CRAE and AA models across 34 global sites. In our prior evaluation studies, the performance of the GG model was quite satisfactory among five commonly used ET models (see details in Supplement 1). Thus, in this study we mainly focus on the GG model as a physical framework to investigate the possibility of deriving a time series of λE_a with only standard meteorological data.

Nevertheless, there are still limitations in the application of the GG model. First, the nonlinear relationship between the relative evapotranspiration ratio and the drying power in Granger and Gray's original work (1989) was derived based on limited data points (158) of λE_a in absence of measurements from wet environments. Thus, its applicability over a wide range of land types and climatic conditions need to be further investigated (Long and Singh, 2010). Secondly, the GG model has mostly been used on a specific timescale, namely monthly (Xu and Singh, 2005; Anayah and Kaluarachchi, 2014), daily (Han et al., 2011) and subdiurnal (Crago and Crowley, 2005). However, systematic comparisons of its performances on different timescales are relatively sparse and its dependence on timescales is not fully understood (Crago and Qualls, 2013). Finally, the arid northwestern China is characterized by a widely distributed Gobi desert interspersed with many oases of different sizes and shapes (Zhu et al., 2014a). Land surface processes of this heterogeneous region are much more complex than in other regions (Wang and Mitsuta, 1992). Thus, the applicability of the GG model in such regions needs to be investigated in details.

In the present study, the objective is to understand and evaluate the performance of the GG model in estimating λE_a at two different timescales (i.e., daily and half-hourly). This effort is achieved by using a collection of high quality eddy covariance flux tower data across a variety of land surface types and conditions in northern China. The main research questions of this study include: (1) determine if the nonlinear relationship between the relative evapotranspiration ratio and the drying power proposed by Granger and Gray (1989) is suitable for different land cover types and climatic conditions; (2) evaluate the performance of the GG model at different timescales, and (3) identify the main sources of uncertainty in computing λE_a using the GG model.

2. Materials and methods

2.1. Study sites

One of the principal limitations in the evaluation of ET models is the availability of accurate and descriptive input forcing data (Baldocchi et al., 2004). The Coordinated Enhanced Observation Project (CEOP) in arid and semi-arid regions in northern China (http://observation.tea.ac.cn/) provides a high-quality dataset of surface fluxes and meteorological data, and makes them an appropriate source for model evaluation. In this study, the model was tested against 12 eddy covariance (EC) flux sites representing a range of vegetation/land cover types in northern China that included cropland, grassland, wetland, desert shrub and forest. These datasets are listed in Table 1. For croplands, two sites (Dunhuang and Daman) are located in the arid northwest China and the others in semi-arid northern China. For grasslands, Arou is an alpine meadow site, Yuzhong represents a typical steppe, Dongsu represents a desert steppe, while Tongyu represents a degraded grassland. For forest and shrub ecosystems, Guantan is a sub-alpine spruce (*P. crassifolia*) forest site, and Ejina represents a typical desert shrub (*Tamarix* spp.). The Maqu alpine wetland is located on the Qinghai-Tibet Plateau and is classified as a semi-humid climatic zone.

2.2. Measurements and data processing

The EC systems were mounted on towers ranging from 2 to 25 m above the various canopy heights (Table 1). Each EC system consisted of a three-dimensional sonic anemometer (CSAT3, Campbell Scientific Inc., UT, USA) that measured instantaneous horizontal (u, v), vertical (w) wind speeds and sonic air temperature fluctuations and an open path infrared gas analyser (Li-7500, LI-COR Inc., USA) that measured the water vapour density and carbon dioxide concentrations fluctuations. The EC instruments were sampled at a frequency of 10 Hz and data were continuously recorded on a data logger (CR5000, Campbell Scientific Inc.). Post-processing calculations were performed using the EdiRe (University of Edinburgh, http://www.geos.ed.ac.uk/abs/research/micromet/EdiRe) software package that included spike detection, lag correction of H_2O/CO_2 relative to the vertical wind component, sonic virtual temperature conversion, planar fit coordinate rotation, the WPL (Webb et al., 1980) density fluctuation corrections and frequency response corrections (Xu et al., 2014). Data gaps (usually no more than 25% of total observations) due to instrument malfunction, power failure and bad weather conditions were filled using an artificial neural network (ANN) and mean diurnal variations (MDV) methods (Falge et al., 2001). The gap-filled daily mean actual latent heat flux (λE_a) by the two methods were quite similar to the observed values (see details in Supplement 1). The energy closure which may be affected by many factors is still a key indicator to assess the quality of the flux data. Liu et al. (2011) examined the energy closure at the different sites of the CEOP sites. Overall, the energy balance closure (the sum of sensible heat and latent heat against available energy) for half-hourly data ranged from 81% to 90% with a mean about 85% across all EC flux towers. On daily basis, the energy balance closure slightly improved and ranged from 85% to 98% with a mean of 92%.

Continuous ancillary measurements also included standard hydro-meteorological variables. These included rainfall (TE525MM, Campbell Scientific Instruments Inc.), air temperature, relative humidity (HMP45C, Vaisala Inc., Helsinki, Finland), wind speed/direction (034B, Met One Instruments Inc., USA), downward and upward solar and longwave radiation (PSP, The EPPLEY Laboratory Inc., USA), soil temperature (Campbell-107, Campbell Scientific Instruments Inc.) and moisture (CS616,

Table 1
Main characteristics of the 12 flux sites in the study region.

Site[a]	Location	Elevation (m)	EC above canopy (m)	Annual precipitation (mm)	Climate zone	Vegetation type	Year	References
Crops								
Dunhuang	39°52′N, 94°06′E	1300	4.5	37	Arid	Irrigated cropland (grape)	2013	Bai et al. (2015)
Daman	38°51′N, 100°22′E	1556	4.5	125	Arid	Irrigated cropland (maize)	2012	Zhu et al. (2014a); Liu et al. (2016)
Changwu	35°12′N, 107°40′E	1220	4	580	Semi-arid	Cropland (maize)	2009	Wang et al. (2010)
Guantao	36°31′N, 115°07′E	42	15	536	Semi-arid	Cropland (wheat)	2009	Xu et al. (2014)
Miyun	40°38′N, 117°19′E	352	25	584	Semi-arid	Cropland (maize)	2009	Xu et al. (2014)
Grasslands								
Arou	38°02′N, 100°27′E	3033	2	396	Semi-arid	Alpine meadow	2008	Zhu et al. (2013, 2014b)
Yuzhong	35°57′N, 104°08′E	1965	2	382	Semi-arid	Typical steppe	2009	Wang et al. (2010)
Dongsu	44°05′N, 113°34′E	990	2	287	Arid	Desert steppe	2009	Wang et al. (2010)
Tongyu	44°34′N, 122°55′E	151	2	404	Semi-arid	Degraded grassland	2009	Wang et al. (2010)
Forest and shrub								
Guantan	38°32′N, 100°15′E	2823	20	360	Semi-arid	Sub-alpine spruce forest	2008	Zhu et al. (2014c)
Ejina	42°02′N, 101°30′E	878	4	37	Arid	Desert shrub	2014	Li et al. (2013)
Wetland								
Maqu	34°00′N, 102°14′E	3423	2	599	Semi-humid	Alpine wetland	2009	Wang et al. (2010)

[a] The sites are grouped by land type. Within each land type, sites are listed from west to east, general aligning with decreasing aridity.

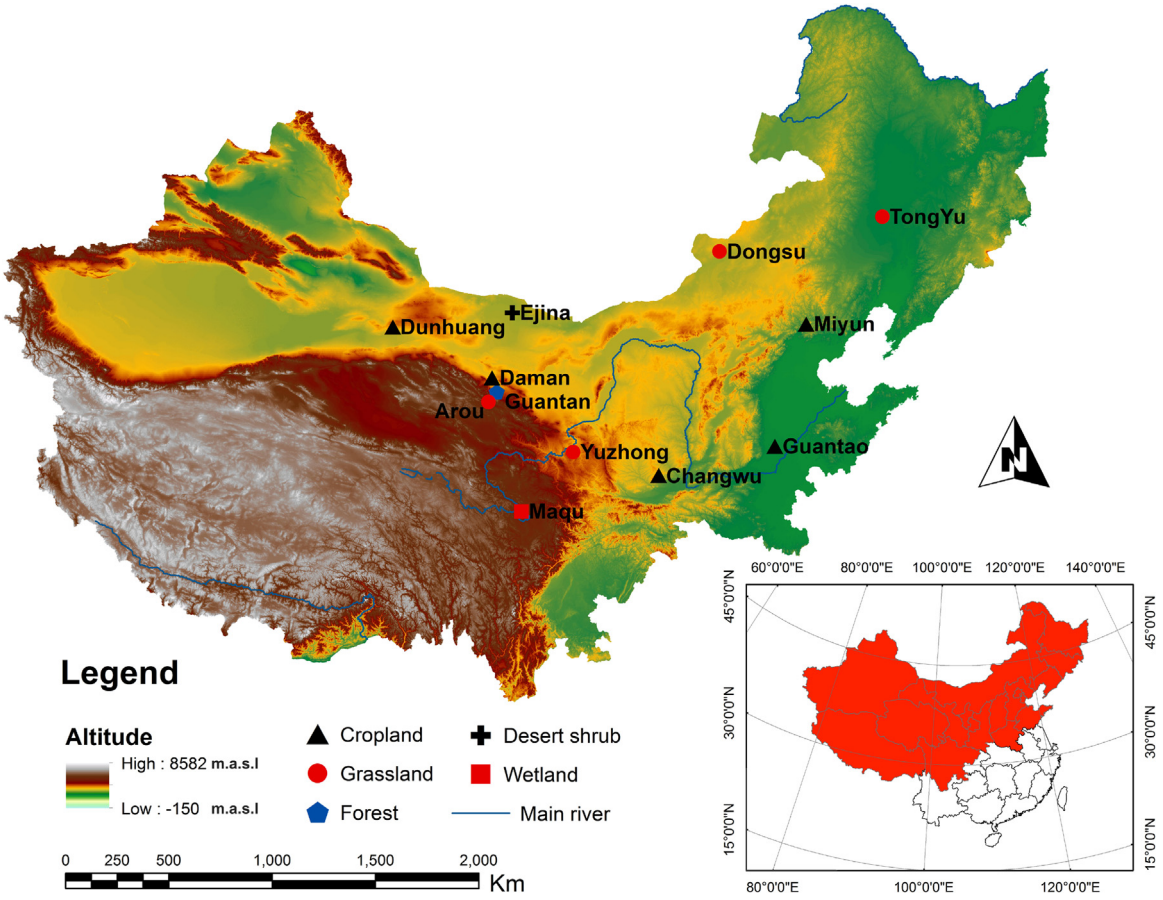

Fig. 1. Location of the eddy covariance towers used to provide forcing and validation data in this study across north China.

Campbell Scientific Instruments Inc.) profiles at 0.02, 0.04, 0.1, 0.2, 0.4, 0.8, 1.2 and 1.6 m depths, and surface soil heat flux at the depth of 0.05 m (HFT3, Campbell Scientific Instruments Inc.). These data were logged every 10 min by a digital micrologger (CR23X, Campbell Scientific Inc.) equipped with an analog multiplexer (AM416) used for sampling and logging data (Fig. 1).

2.3. Model descriptions

The asymmetric CR in the GG model can be expressed as (Granger, 1989; Granger and Gray, 1989; Szilagyi, 2007):

$$\lambda E_a + \frac{\gamma}{\Delta}\lambda E_{w,mt} = \left(1 + \frac{\gamma}{\Delta}\right)\lambda E_p \quad (1)$$

where λE_a represents the actual evapotranspiration rate from a homogeneous area ($W\,m^{-2}$); λE_p is the maximum possible evapotranspiration rate that would occur under the actual meteorological and energy conditions if only the available energy were the limiting factor ($W\,m^{-2}$); $\lambda E_{w,mt}$ is the mass transfer evapotranspiration from wet surface ($W\,m^{-2}$), which is governed by the unknown wet surface temperature (T_{ws}; °C); Δ is the slope of the saturation vapor pressure curve at the air temperature ($kPa\,K^{-1}$), and γ is the psychrometic constant ($kPa\,K^{-1}$); Eqn. (1) shows that for constant available energy and atmospheric conditions the CR is not asymmetric for cases where $\gamma/\Delta \neq 1$. In the GG model, λE_p was estimated using the Penman (1948) combination equation:

$$\lambda E_p = \frac{\Delta}{\Delta+\gamma} Q_n + \frac{\gamma}{\Delta+\gamma}\lambda E_{aero} \quad (2)$$

in which, $Q_n = R_n - G$ is available energy ($W\,m^{-2}$); R_n is the net radiation ($W\,m^{-2}$); G is soil heat flux ($W\,m^{-2}$), and λE_{aero} ($W\,m^{-2}$) is the drying power of the air, which represents the capacity of the atmosphere to transport the water vapour from surfaces. When applying the Penman (1948) equation for the short-term (e.g., half-hourly) period, the effect of atmospheric stability, which varies through the day, can be important in the formulation of λE_{aero} (Brutsaert, 2005). In this study, λE_{aero} was calculated on the basis of the Monin-Obukhov similarity (MOS) theory (Monin and Obukhov, 1954) according to Brutsaert (1982) and Parlange and Katul (1992):

$$\lambda E_{aero} = \frac{\rho_a c_P}{\gamma} \frac{k u_* (e_a^* - e_a)}{[\ln(\frac{z-d_0}{z_{0v}}) - \psi_v(\frac{z-d_0}{L})]} \quad (3)$$

where ρ_a is the density of the air ($kg\,m^{-3}$); c_P is the specific heat of air at constant pressure ($J\,kg^{-1}\,K^{-1}$); $k = 0.4$ is the von Karman constant; u_* is the friction velocity ($m\,s^{-1}$); e_a^* and e_a are the saturated vapor pressure at air temperature and actual vapor pressure of the air (kPa), respectively; z is the measurement height (m); d_0 is the displacement height (m), computed as 0.7 times the vegetation height (z_{veg}); z_{0v} is the scalar roughness height for water vapor; ψ_v denotes the stability function for water vapor (Businger, 1988; Dyer, 1974), and L is the Obukhov length (m) defined as:

$$L = \frac{-u_*^3}{kg[H_v/(\rho_a c_p T_a)]} \quad (4)$$

where g is gravitational acceleration ($9.81\,m\,s^{-2}$); T_a is the air temperature (K); H_v is the specific flux of virtual sensible heat ($H_v = H + 0.61 T_a c_p \lambda E_a$), and H is the sensible heat flux ($W\,m^{-2}$), which can be computed from the surface energy balance:

$$H = Q_n - \lambda E_a \quad (5)$$

Following Brutsaert (1982), u_* can be estimated from the measured horizontal wind speed (U; $m\,s^{-1}$) using the MOS profile equation:

$$u_* = \frac{kU}{\ln(\frac{z-d_0}{z_{0m}}) - \psi_m(\frac{z-d_0}{L})} \quad (6)$$

where z_{0m} is the roughness height for momentum (m), and is computed as $0.1 z_{veg}$(Dingman, 2002), and $\psi_m$denotes the stability correction function for momentum (Businger, 1988; Dyer, 1974). A complete description of the stability functions for ψ_m and ψ_v is presented in Supplement 2. Further, the roughness height for water vapor (z_{0v}) is estimated using the so-called kB^{-1}approach (Crago and Suleiman, 2005; Crago et al., 2010) relating the momentum (z_{0m}) and scalar (z_{0v}) roughness heights to the roughness Reynolds number R_{e*} as follows (Salvucci and Gentine, 2013):

$$kB^{-1} = \ln(z_{0m}/z_{0v}) \simeq k(6R_{e*}^{1/4} - 5) \quad (7)$$

In Eqn. (7), the roughness Reynolds (R_{e*}) is defined as $u_* z_{0m}/\upsilon$, where υ is the kinematic viscosity, being about $1.45 \times 10^{-5}\,m^2\,s^{-1}$. Here, the roughness Reynolds number R_{e*} is given as 5.7 for water vapor according to Salvucci and Gentine (2013). Submitting this number into Eqn. (7) yields the kB^{-1} of 1.7. This value falls in the range of 1.5–3, which is often assumed for practical calculations (Brutsaert, 1982; Allen et al., 1998; Crago et al., 2010).

To exclude the unknown wet surface temperature variable (T_{ws}; °C), Granger and Gray (1989) introduced the concepts of relative evapotranspiration ($\Phi = \lambda E_a/\lambda E_{w,mt}$) and the relative drying power ($D = \lambda E_{aero}/(\lambda E_{aero} + Q_n)$) which reflects to an extent the dryness of the surface. The relationship between Φ and D has been proposed as (Granger, 1989):

$$\Phi = \frac{1}{1 + ce^{mD}} \quad (8)$$

where c and m are fitting parameters, which determine the response properties of Φ to D (Granger and Gray, 1989; Xu and Singh, 2005). Using data monitored at two stations in the semi-arid climate zone of western Canada, Granger and Gray (1989) estimated $c = 0.028$ and $m = 8.045$ in absence of measurements from wet environments ($\Phi > 0.7$). Substituting the Penman (1948) equation (Eqn. (2)) and the relative evapotranspiration ($\lambda E_{w,mt} = \lambda E_a/\Phi$) into Granger and Gray's (1989) CR model (Eqn. (1)) yields the general expression for evaporation from a non-saturated surface as:

$$\lambda E_a = \frac{\Delta \Phi Q_n}{\Delta\Phi + \gamma} + \frac{\gamma \Phi \lambda E_{aero}}{\Delta\Phi + \gamma} \quad (9)$$

At the daily timescale, the atmospheric stability is assumed to be neutral such that $\psi_m = 0$ and $\psi_v = 0$(Brutsaert, 2005). At the half-hourly timescale, the method from which to calculate λE_a includes Eqns. (3)–(9). The unknowns in this system are λE_a, λE_{aero}, H, D, L and u_*, which is solved using an iterative procedure with a closure specification of $0.1\,W\,m^{-2}$ on λE_a (see details in Supplement 2).

2.4. Performance metrics

All data from the different sites were obtained on a half-hourly basis, and were processed into their daily mean values according to the procedures proposed by Allen et al. (1998). The performance of the GG model on two different timescales (i.e., half-hourly and daily) was quantified by using the correlation coefficient (R^2), slope (b_0) and interception (b_1) of the Deming regression line ($y = b_0 x + b_1$) between the measured (x) and estimated (y) values (Deming, 1943). Model-data mismatch was also evaluated using the root mean square error (RMSE), normalized mean absolute error (NMAE) and the index of agreement (IA) of model efficiency (Legates and McCabe, 1999; Poblete-Echeverria and Ortega-Farias, 2009). These were calculated as:

$$RMSE = \sqrt{\frac{1}{n}\sum_{t=1}^{n}[O(t) - M(t)]^2} \quad (10)$$

$$NMAE = \frac{\sum_{t=1}^{n}|O(t) - M(t)|}{n\overline{O}} \quad (11)$$

$$IA = 1 - \frac{\sum_{t=1}^{n}[O(t) - M(t)]^2}{\sum_{t=1}^{n}[|O(t) - \overline{O}| + |M(t) - \overline{O}|]^2} \quad (12)$$

where n is the total number of observations; $O(t)$is the observed values at time t, $\overline{O}$ is the mean of the observed data, and $M(t)$is the individual model predictions at time t. The index of agreement (IA)

is the ratio of the mean square error and the potential error (the largest value that the squared difference of each pair can attain). The value of IA varies between 0 and 1 where a value of 1 represents perfect agreement between O and M and 0 describes complete disagreement.

3. Results

3.1. Model-data agreement on daily timescale

Comparisons between modeled and observed λE_a on a daily timescale are presented in Table 2 and Fig. 2. For the cropland surfaces, the GG model was able to predict the daily mean λE_aover the three crops grown in semi-arid regions (i.e., Miyun, Guantao and Changwu). The model fit to the observed data for these three crops ranged for Deming regression line slope (b_0) from 1.06 to 1.11, and for the correlation coefficient (R^2) from 0.61 to 0.82 (Table 2). However, the model underestimated the daily mean λE_a for the other two irrigated crops in the arid region (i.e., Daman and Dunhuang). The value of b_0 was 0.63 and 0.45, and the corresponding R^2 was 0.56 and 0.38 for Daman and Dunhuang, respectively (Table 2 and Fig. 2a).

For grassland ecosystems, the daily mean λE_a were well quantified by the model (Fig. 2b) with high IA (>0.84) and small NMAE (<0.33). The value of b_0 varied between 0.78 and 1.05 with an average of 0.92, and the corresponding R^2 ranged from 0.65 to 0.83 with a mean about 0.72. For the wetland surface, the slope of the linear regression was very close to one (1.06; Table 2) with NMAE and IA values close to zero and 1.0, respectively.

For the sub-alpine spruce forest ecosystem, the predictions were also comparable to the measurements with values of b_0, R^2, NMAE and IA equal to 0.70, 0.57, 0.30 and 0.78, respectively. However, occasional underestimations were observed, which mainly occurred during four dry periods (discussed below). For the desert shrub ecosystem, the model had a very low performance, and tended to underestimate the mean daily λE_a (Fig. 4d). The values of b_0, R^2, NMAE and IA was 0.09, 0.14, 0.63 and 0.48, respectively (Table 2).

3.2. Model-Data agreement on half-hourly timescale

For the half-hourly timescale, the model performance was generally better than that for the daily timescale, and overall satisfactory for the 12 tower sites across north China (Table 2 and Fig. 3). For the two crops in the arid region, the value of b_0 increased from 0.45 and 0.63 on the daily timescale to 0.89 and 1.05 on the half-hourly timescale for Dunhuang and Daman, respectively, and the corresponding R^2 from 0.38 and 0.56–0.76 and 0.81 (Table 2). However, underestimations were also observed for the two arid crops when λE_a was greater than 600 W m^{-2} (Fig. 3a). For grassland ecosystems, the model performances on half-hourly timescales were acceptable and slightly better than that on daily timescales. As shown in Fig. 3b, modeled data were fitted to the measured data ranged in b_0 values of 0.92–1.12, and an R^2 of 0.54–0.81 (Table 2). For the wet land, the model performed reasonably well with b_0, R^2 and IA equal to 1.09, 0.75 and 0.93, respectively, and the modeled half-hourly latent heat fluxes generally clustered well with the measured values (Fig. 3c). For the forest ecosystem, the value of $b_0$and R^2 for the half-hourly timescale was 0.77 and 0.64, respectively, which was close to the daily timescale (i.e., 0.70 and 0.57). For the desert shrub ecosystem, the model performance for the half-hourly timescale was quite good with values of b_0, R^2 and IA equal to 0.93, 0.64 and 0.93, respectively. Comparing with the model performance on the daily timescale, significant underestimation was not observed on the half-hourly timescale, indicating that the model performed differently on different timescales and that dependence on timescales need to be further investigated (Crago and Qualls, 2013).

To investigate the causes of the underestimations over the two arid crops (i.e., Daman and Dunhuang), the diurnal traces of R_n, H and λE_a (measured and modeled) over the two arid crops on selected clear days are presented in Fig. 4. Resulting from the high surface heterogeneities in the arid northwest China, the special phenomenon known as the "oasis effect" (Oke, 1978; Wang and Mitsuta, 1992) was observed and is characterized as: (1) H is very small and even negative (downward) in the day time especially in the afternoon (Fig. 4) because of horizontal advection of hot dry air originating over the desert to a cropland surface; (2) measured λE_a can often exceed or equal R_n due to the added energy in the form of downward sensible heat flux (Evett et al., 2012; Zhu et al., 2014a). Under such conditions, the model significantly underestimated the actual λE_a values as it does not have the ability to account for the advection of the vapour pressure deficit. Thus, a parameter is needed to properly characterize the horizontal advection process in the ET model when used in heterogeneous landscapes in future studies.

3.3. Relationship between dailyΦ **and** D

The measurements from climatically, hydrologically and biophysically diverse sites across northern China provided a wide range in the daily Φ ($= \dfrac{\gamma\lambda E_a}{\Delta Q_n + \gamma\lambda E_{\text{aero}} - \Delta\lambda E_a}$) and D values (Fig. 5). The results indicated that the expression proposed by Granger and Gray (1989) is applicable to most ecosystems across northern China including the four grasslands, the sub-alpine spruce forest, the wet land and the three croplands in semi-arid regions (Fig. 5). For the two croplands in the arid northwest China, the values of Φ varied from 0.08 to 0.94 with D from 0.39 to 0.94. The values of Φ were greater than that predicated by the Granger and Gray's (1989) equation due to the enhanced λE_a by horizontal advection (Fig. 5). The wide range in Φ and D allows to develop the functional relationship between them with confidence. The least-square estimation of parameters c and m in Eqn. (8) for cropland in arid northwest China was 0.016 and 6.679, respectively. For the desert shrub, the values of D were clustered above 0.8 and Φ below 0.2 (Fig. 5), reflecting the relative dry climate conditions for this region (Carey et al., 2005). It was also observed that these data fell above the curve of Granger and Gray (1989), which is probably due to the enhanced λE_a by plant transpiration maintained by direct deep root water uptake (beneath 1.2 m depth; data not shown) of the desert shrub (Jackson et al., 2000). Based on the relative narrow range in Φ, the estimated parameters of c and m for desert shrub was 0.001 and 10.426, respectively.

Using the recalibrated parameters for the two croplands in arid northwest China ($c = 0.016$ and $m = 6.679$) and the desert shrub ($c = 0.001$ and $m = 10.426$), we recomputed the latent heat fluxes on daily and half-hourly timescales. For the daily timescale, the model performance using the recalibrated parameters was improved relative to the original parameters proposed by Granger and Gray (1989) (Fig. 6). The values of R^2 increased from 0.38, 0.56 and 0.14 (original parameters) to 0.78, 0.78 and 0.70 (recalibrated parameters) for Dunhuang, Daman and Ejina, respectively. For the two arid croplands, the values of b_0 were close to 1 (1.05 and 1.08 for Dunhuang and Daman, respectively; Fig. 6a and b), and the effects of local advection process on λE_a seemed to be implicitly accounted for by using the recalibrated parameters. For the desert shrub ecosystem, the performance of the model with recalibrated parameters was variable in daily simulation. For instance, it overestimated the latent heat fluxes when the daily mean λE_a was less than 60 W m^{-2}, while it underestimated the latent heat fluxes when

Table 2
A summary of the performance of the GG on different time scales for different land surface type across north China.

Sites	Daily basis							Half-hourly basis						
	n	b_0	b_1	R^2	RMSE	NMAE	IA	*n*	b_0	b_1	R^2	RMSE	NMAE	IA
Crops														
Dunhuang	52	**0.45**	−4.00	**0.38**	92.0	0.57	0.52	4785	0.89	4.24	0.76	99.9	0.47	0.92
Daman	66	**0.63**	0.43	0.56	55.5	0.39	0.60	3168	1.05	0.79	0.81	87.1	0.51	0.93
Changwu	53	1.06	−9.45	0.61	22.3	0.33	0.80	3613	0.91	−9.27	0.54	52.2	0.66	0.85
Guantao	57	1.11	−24.5	0.68	24.5	0.25	0.79	4781	1.14	−0.15	0.74	70.4	0.61	0.89
Miyun	36	1.09	−12.4	0.82	24.0	0.25	0.82	3629	1.11	−5.54	0.73	76.1	0.62	0.91
Grasslands														
Arou	117	0.87	−1.82	0.83	17.7	0.17	0.94	4470	1.06	−19.3	0.81	67.5	0.58	0.93
Yuzhong	86	0.78	3.19	0.65	22.7	0.33	0.84	5134	1.06	−9.43	0.54	67.4	0.82	0.82
Dongsu	61	1.05	−8.95	0.76	13.9	0.24	0.93	3870	0.92	0.06	0.59	27.4	0.67	0.85
Tongyu	56	0.98	6.76	0.75	16.7	0.26	0.92	4287	1.12	−12.3	0.56	71.8	0.78	0.85
Forest and shrub														
Guantan	80	0.70	11.8	0.57	25.7	0.30	0.78	5706	0.77	−6.78	0.64	66.6	0.62	0.89
Ejina	112	**0.09**	32.0	**0.14**	72.1	0.63	0.48	3280	0.93	−3.57	0.64	82.9	0.43	0.93
Wetland														
Maqu	38	1.06	−5.35	0.89	17.0	0.16	0.90	3448	1.09	−5.60	0.75	61.8	0.50	0.93

n: Number of observations. b_0, b_1: The slope and intercept of the Deming regression line between measured and simulated values. Bold numbers show the slope of the Deming regression line is significantly different from 1 and R^2 lower than 0.5.

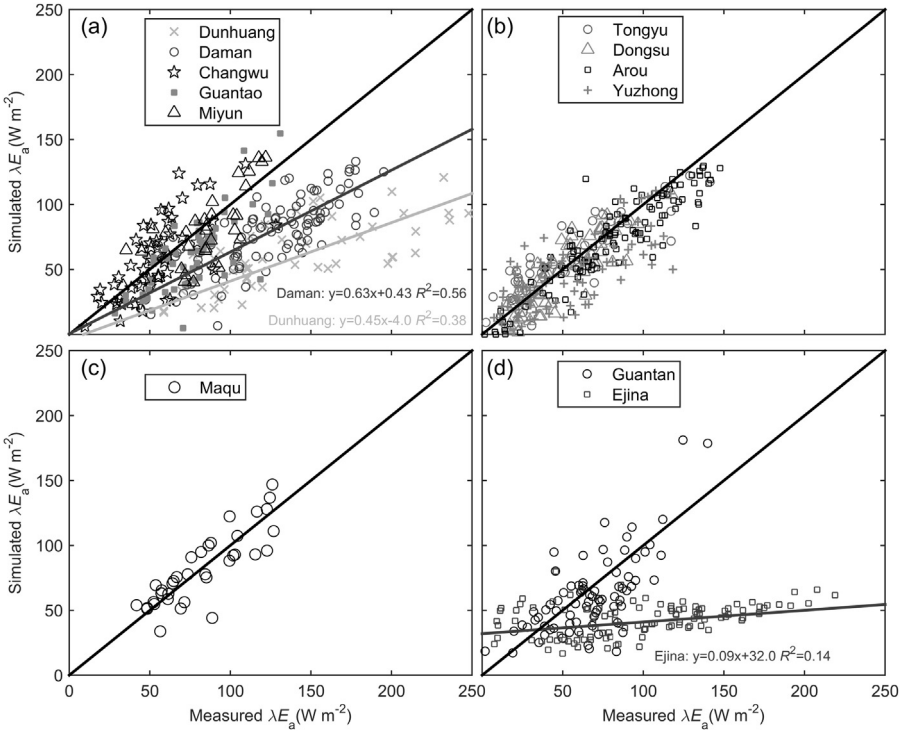

Fig. 2. Regression between measured and simulated λE_a on daily timescale for different land cover types. (a) cropland; (b) grassland; (c) wetland; and (d) forest and desert shrub land.

the daily mean λE_a was larger than 150 W m^{-2}. This result indicates that challenges remain to accurately estimate the latent heat fluxes over sparse deep root ecosystems in arid regions (Domingo et al., 1999).

On half-hourly timescale, no significant differences were observed in model performances between using the original and the recalibrated parameters (Fig. 6). To better understand these results, sensitivity analysis of the GG model to parameters on different timescales was performed (see details in Supplement 3). As shown in Fig. 7, the model output in λE_a on a daily timescale is sensitive to the changes in both parameters (i.e., a 50% decrease in parameter *m* leaded to a 250% increase in λE_a, where a 50% increase in *m* caused nearly 80% decrease in λE_a; and a 50% decrease in parameter *c* leads to a 50% increase in λE_a, where a 50% increase in parameter *c* caused nearly 20% increase in λE_a). On the other hand, sensitivity of the model output on half-hourly timescale was generally less than 0.5% with increase/decrease in parameters by 50%.

3.4. Relationship between daily λE_a and SWC

Soil moisture has significant impact on λE_a in water-limited environments (Seneviratne et al., 2010). Model predictions of actual λE_a in such regimes requires the model be sensitive to the rapid changes in soil water content (SWC; %) (Teuling et al., 2006). Two natural ecosystems (i.e., the grassland in Yuzhong and the sub-

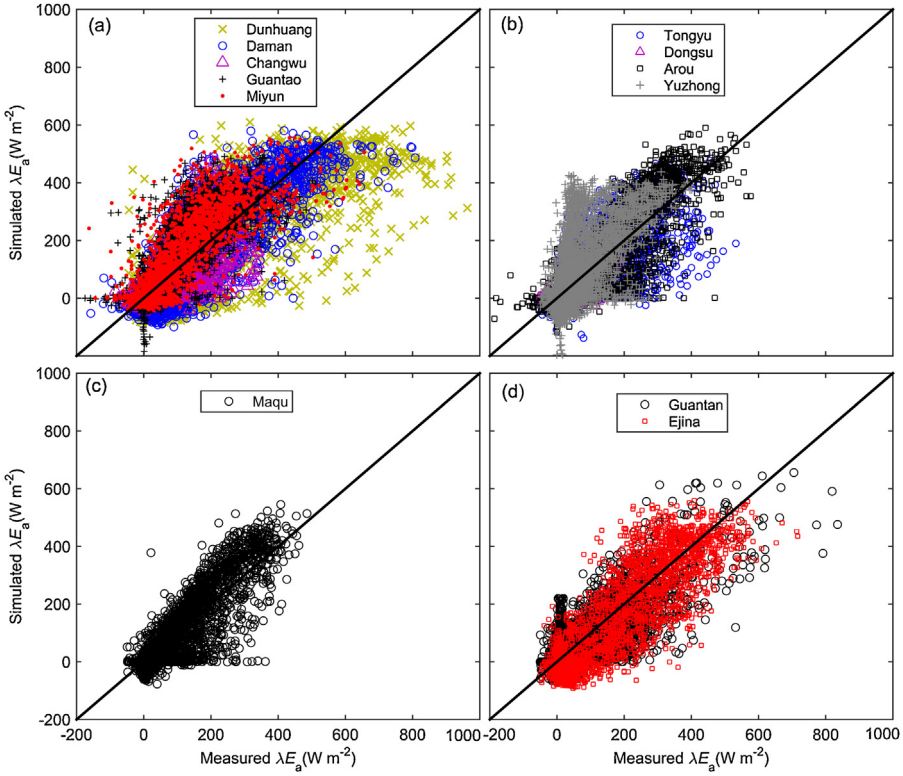

Fig. 3. Regression between measured and simulated λE_a on half-hourly timescale for different land cover types. (a) cropland; (b) grassland; (c) wetland; and (d) forest and desert shrub land.

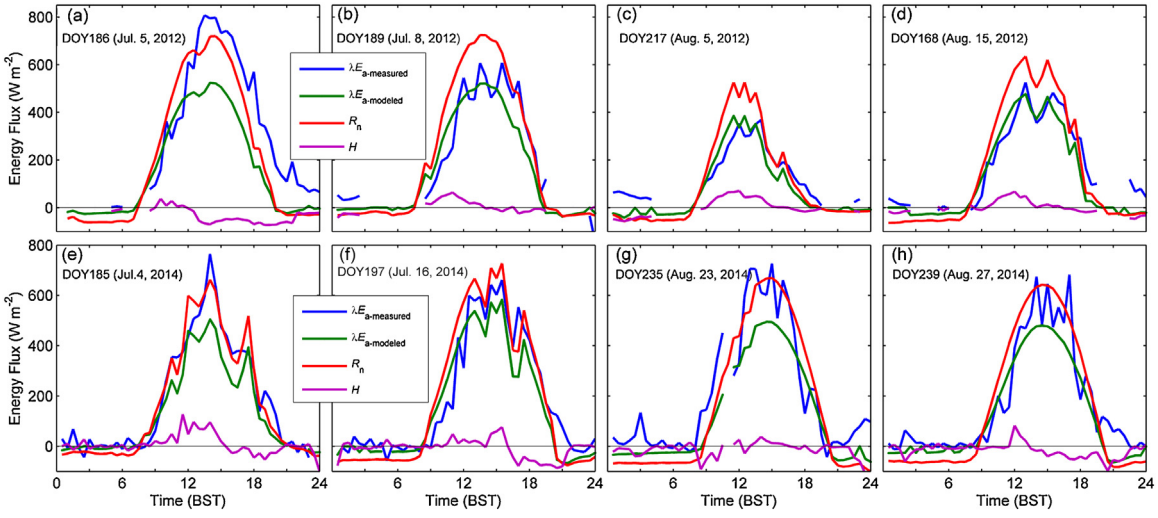

Fig. 4. Diurnal variations in R_n, H, and modeled and measured λE_a over cropland ecosystems in arid northwest China. (a–d) represent observation at Daman station; and (e–f) represent observation at Dunhuang station.

alpine spruce forest in Guantan) were selected to evaluate the responses of the model to changes in SWC. A time series of daily mean λE_p, λE_{aero}, D, λE_a (measured and simulated) and SWC measured at 5 cm depth are illustrated in Fig. 8. For the forest ecosystem, four dry periods (DOY163-167, DOY187-202, DOY236-246, and DOY253-259) and one wet period (DOY227-231) were observed (Fig. 8e). During the dry periods, the values of D and λE_{aero} were relative high varying from 0.46 to 0.90 with a mean of 0.77 and from 148.7 W m^{-2} to 1315.3 W m^{-2} with a mean of 679.7 W m^{-2}, respectively. During the wet periods, the D values were small ranging from 0.14 to 0.34 with a mean 0.22, and the values of λE_{aero} nearly approached zero ranging from 12.4 W m^{-2} to 114.1 W m^{-2} with a mean of 38.1 W m^{-2} (Fig. 8b and c). It was observed that the fluctuation of measured daily mean λE_a from the forest ecosystem during the dry periods should be attribution to the Q_n (data not shown due to its similar pattern to λE_p; Fig. 8a) rather than surface soil moisture (Fig. 8a, d and e). The average value of daily mean λE_a during the dry periods (being 72.6 W m^{-2}) was even slightly higher than that during the whole study period (66.8 W m^{-2}). Thus, the forest ecosystem may maintain evapotranspiration during the dry periods by utilizing deep water resources (Kelliher et al., 1993).

For the grassland ecosystem in Yuzhong, significant increase in SWC was observed after 2 August (DOY214) because of summer monsoon rains (Fig. 8j). The values of D varied from 0.46 to 0.93

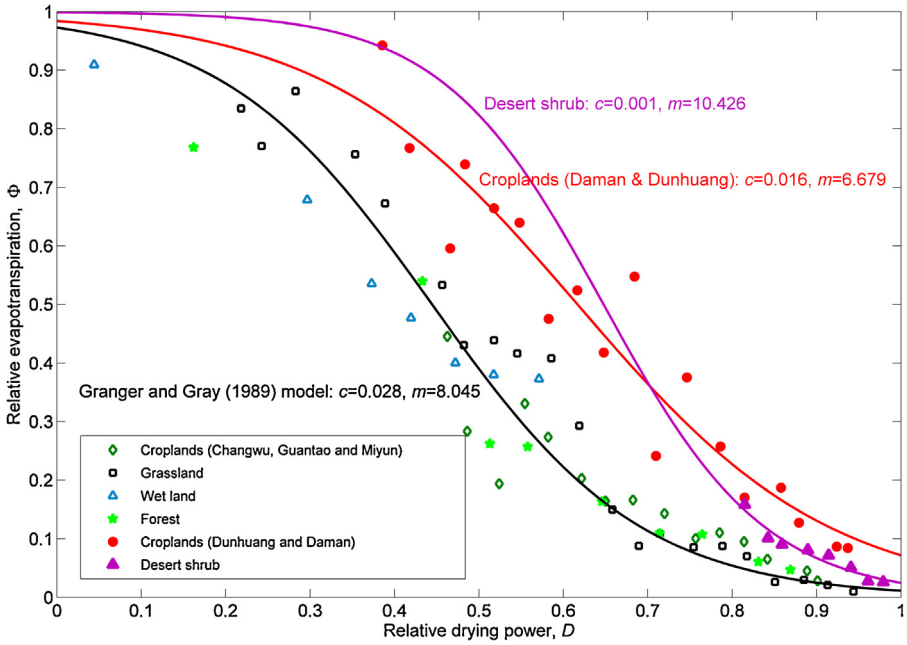

Fig. 5. Plot of mean daily relative evapotranspiration (Φ) against mean daily relative drying power (D) for different sites across north China.

with a mean of 0.76 and from 0.14 to 0.79 with a mean of 0.56 for the dry and wet periods (Fig. 8h), respectively. The mean values of λE_{aero}decreased from 370.8 W m^{-2} during the dry period to 126.8 W m^{-2} during the wet period (Fig. 8 g). The responses of measured D and λE_{aero} to SWC were in agreement with the theoretical hypothesis of Granger and Gray's (1989) model, and fairly robust prediction accuracy on seasonal variation of daily mean λE_a over these two ecosystems was obtained (Fig. 8d and i; Table 2).

4. Discussions

This study serves as prime examples of potentially useful for robustly and accurately predicting the actual evapotranspiraiotn on daily and half-hourly timescales by the GG model. Recently, Huntington et al. (2011) applied a modified Brutsaert and Stricker (1979) advection-aridity model to estimate monthly and annual evapotranspiration from arid shrublands of Southwestern United Sates, and quite satisfactory prediction accuracy were obtained. Salvucci and Gentine (2013) also proposed to estimate the λE_a by minimizing the variance of the diurnal cycle of relative humidity profile from meteorological data. The common characteristics of these approaches are that they require only the routine meteorological measurements to estimate λE_a without detailed knowledge of the surface biophysical and hydrological states. It can be suspected that they will have a wide application in understanding and predicting hydrological cycle in the context of climate change (Seneviratne et al., 2010; Huntington et al., 2011), and play a role in hydrology for years to come (Crago and Qualls, 2013). In the future, more works on the performance intercomparisons of these approaches across a wide range of hydrological, climatic, and biophysical sites may be needed.

The responses of forest canopy evapotranspiration to drought in this study are consistent with previous findings (Baldocchi et al., 2004). For example, Nepstad et al. (1994) reported that the Amazonian evergreen forests maintain evapotranspiration during five-month dry periods in 1992 by absorbing water from the soil to depths of more than 8 m. Baldocchi et al. (2004) illustrated that the ability of some roots to absorb deep soil water (below 0.6 m) ensures the oak trees (*Quercus douglasii*) in savannas to maintain transpiration during the summer dry period. Teuling et al. (2010) observed that λE_a over Europe forest during summer heatwave days is similar to that during normal conditions. For the desert shrub in Ejina, the measured cumulative evapotranspiration (520 mm) during the study period far more exceeded the cumulative precipitation (7.4 mm), indicating consumption of water resources in deep soil layer. Thus, significant underestimations of daily mean λE_a over the desert shrub in Ejina (Fig. 2d) were also suspected to be attributed to the combination of relative high wind speed and dry atmospheric boundary conditions (which resulted in very high D values ranging from 0.74 to 0.99 with a mean of 0.90; Fig. 5) and the ability of some roots to tap deep soil water (below 1.2 m; data not shown). Si et al. (2005) reported that the variations in monthly total evapotranspiration over the shrub ecosystem in Ejina were not positively correlated with surface soil moisture. In addition, the performance of two-layer Shuttleworth and Wallace (1985) model was evaluated in Ejina. Also, significantly underestimations of daily evapotranspiration were observed when the canopy and soil surface residences were parameterized using the top layer (0- to 5-cm) SWC (Supplement 1). In the GG model, evapotranspiration direct from deep soil water trough plant root water-uptake cannot be properly distinguished from surface soil water (Wang and Dickinson, 2012), which may ultimately cause some underestimations of λE_a. Therefore, it may still be challenging to properly describe the biological constraints on ET processes over deep root ecosystems in arid environments (Manzoni et al., 2013), and a better understanding in the interactions and feedback mechanisms of plant's physiological properties (e.g., stomatal conductance, leaf area index, rooting distribution, hydraulic architecture; McDonald and Davies, 1996; Jackson et al., 2000) and environmental factors (e.g., soil properties, precipitation, radiation and temperature; de Rosnay and Polcher, 1998; Hoffmann and Jackson, 2000) is still needed.

The GG model has been applied mostly at specific timescales (e.g., monthly, daily and subdiurnal) but comparisons of its performances on different timescales are relatively rare or nonexistent. Thus, the dependences of the model performance on its timescales are not fully understood (Crago and Qualls, 2013). It is known that the original GG model is usually used at daily timescale. In this study, we applied it on subdiurnal time steps by accounting

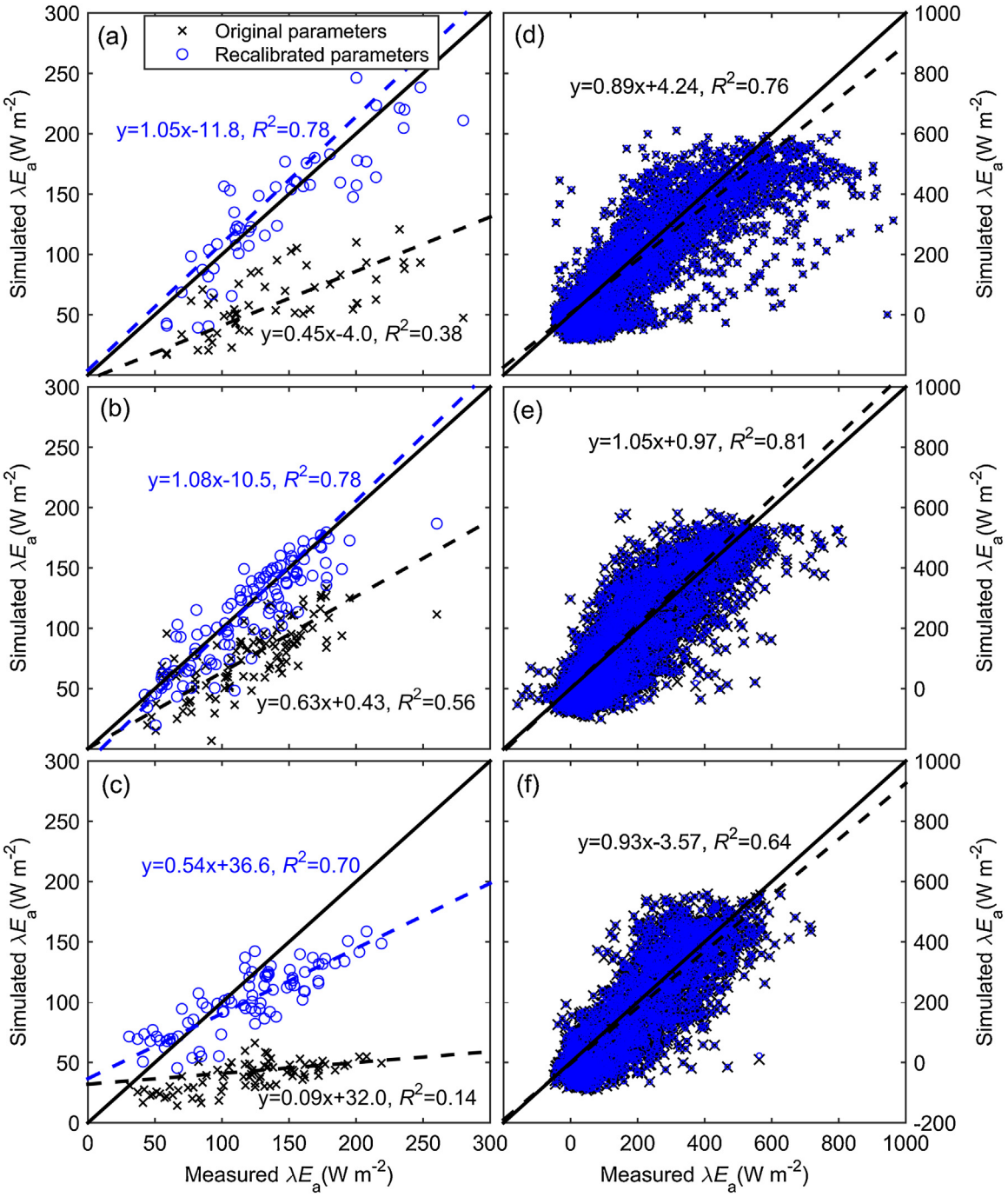

Fig. 6. Regression between measured and simulated λE_a using recalibrated and original parameters for (a) Dunhuang, (b) Daman, and (c) Ejina on daily timescale; and for (e) Dunhuang, (f) Daman, and (g) Ejina on half-hourly timescale.

for atmospheric stability through MOS theory (Brutsaert, 1982; Parlange and Katul, 1992; Katul and Parlange, 1992). It was very interesting to find that the model performances on half-hourly timescale were generally better than that on daily timescale (Table 2), which is consistent with the finding by Vesala et al. (2010). They reported that the predictions of a dynamic vegetation model (ORCHIDEE) were similar to observations on half-hourly timescale, but the predictions were significantly biased on daily timescale (Vesala et al., 2010). This may be due to the fact that the thermodynamic characteristics between the surface and boundary layer on half-hourly timescale were well described by using the MOS theory with a surface energy balance constraint (Eqn. (5)) (Salvucci and Gentine, 2013), while the changes in air characteristics at the reference height when the surface dries out were ignored on daily timescale (Lhommea and Guilioni, 2006). Additionally, the simulated λE_a on half-hourly timescale was far less sensitive to model parameters (cand m) comparing to that on daily time step (Fig. 7 and Supplement 1), which indicated that the performances of the GG model on half-hourly time steps were more robust than that on daily time steps. Therefore, to use the tight coupling property of the land and atmosphere as a means to estimate evapotranspiration, it seems that the meteorological forcing data should be in high temporal resolution.

The main restriction on the CR-based ET models is that they are valid only when there is no horizontal advection from upwind of the evaporating surface (Crago and Qualls, 2013). Resulting from the

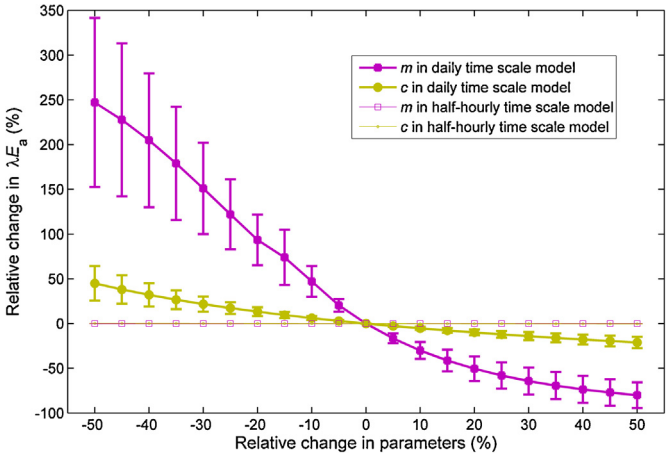

Fig. 7. Changes in daily and half-hourly λE_a in response to changes in parameters c and m with maximum, minimum and mean for the 12 flux tower sites at each perturbation of the parameters (5% within the limits of ±50%). High-low lines on the plot represent the maximum and minimum variations of the 12 sites, and continuous lines represent the mean variation.

high surface heterogeneities, advection was often observed in arid northwest China (e.g., Daman and Dunhuang). Thus, another concern is whether the GG model can be applied to these conditions? Here, we found that it was possible to properly account for advection by adjusting model parameters on daily time steps (Fig. 6a and b). On the contrary, no satisfactory results were obtained by doing so on half-hourly time steps (Fig. 6d and e), partly due to its low sensitivity to parameters (Fig. 7). In Principle, the CR is based on the fact that the dryness of the surface can be inferred from the boundary layer humidity and temperature gradients (Crago and Crowley, 2005). However, under advection conditions with negative latent heat flux (Fig. 4), the validity of the assumptions on which the GG model is developed becomes questionable (e.g., De Bruin et al., 2005; Tolk et al., 2006a,b). Furthermore, the predictive power of the model decreases in moving toward regions of increased heterogeneity (i.e., from Daman to Dunhuang with oasis area being 480 km^2 and 2800 km^2, respectively; Fig. 2a). To account for advection, a modified AA model was proposed by Parlange and Katul (1992). Operationally, the symmetry CR is corrected by adding the absolute value of the negative H_p ($=Q_n - \lambda E_p$) to the wet surface evaporation term (see details in Supplement 1). However, underestimates and slight overestimates by the modified AA model were found at these two sites on daily and half-hourly time steps, respectively (Supplement 1). In addition, the overall performances of the modified AA model were not superior to the GG model with locally-calibrated parameters (Supplement 1). Pettijohn and Salvucci (2006) also reported that the modified AA model increases error in λE_a estimations comparing to the original AA model. Thus, we deduced that it may be more proper to account for advection by using two-dimensional atmospheric models of the dry-wet interface (Pettijohn and Salvucci, 2009; Szilagyi and Jozsa, 2009a,b).

Finally, the lack of closure in energy balance (~15% and 8% on half-hourly and daily timescales, respectively) at EC towers can result in underestimation of latent heat flux. According to previous studies (Lee, 1998; Foken, 2008; Foken et al., 2010), the energy transport with larger eddies which cannot be captured by the EC method may be one of the main causes of the energy imbalance. Thus, area-averaging measuring systems such as large aperture scintillometer (LAS) and airborne sensor might be able to close the surface energy balance better than the EC method (Foken et al., 2010). Liu et al. (2011, 2013) systematically compared the differences between latent heat flux measured by the LAS and EC systems at some CEOP sites. They found that when energy balance closure was larger than 75% the EC-measured latent heat fluxes were very close to the LAS data, with only a 8% difference (Liu et al., 2011, 2013). Thus, the measurements by the EC system were reasonable and thus suitable for comparison with the CR results. However, the non-closure issue remains unresolved at present and special attentions still needed to come to a final solution (Foken et al., 2010).

5. Conclusions

This study presented here demonstrated the potential for estimating λE_a on different timescales (i.e., daily and half-hourly) based on only routine meteorological variables by using the GG model. The results indicated that the GG model is suitable to estimate daily λE_a over most ecosystems in north China with the exceptions of two arid croplands and one desert shrub in northwest China, which

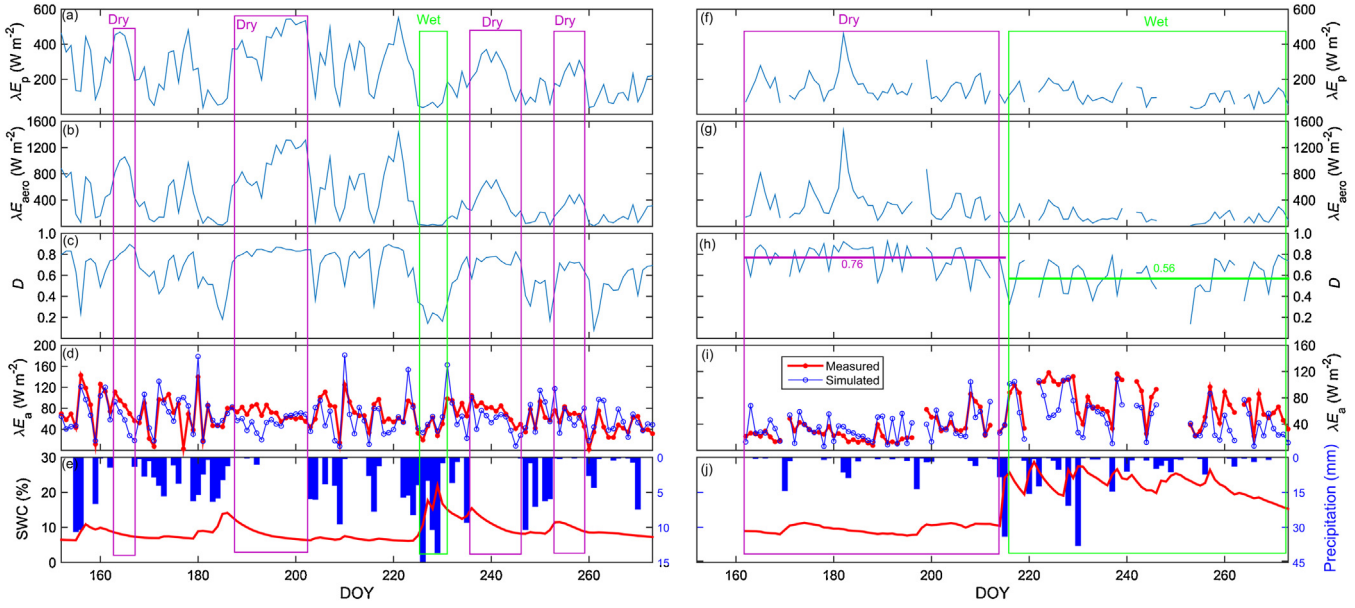

Fig. 8. Comparison between the time series of λE_p, λE_A, D, measured and simulated λE_a, and soil water content (SWC) at 5 cm depth.

may be due to its neglecting the influence of horizontal advection and deep water-uptake by plant roots on the ET process by the GG model. By using the MOS theory with a surface energy balance constraint, the model performances using the original parameter values on half-hourly timescale were generally better than on daily timescale and were quite satisfactory for the 12 tower sites. Thus, further investigation of the timescale dependence of the CR-based ET models is still needed.

Acknowledgements

The authors would thank Prof. Nathaniel Brunsell (associate editor) for his continued help during the revisions of the paper. We also thank the three anonymous reviews for their critical reviews and helpful comments. This research was supported by National Natural Science Foundation of China (nos. 41571016 and 31370467), the One Hundred Person Project of the Chinese Academy of Sciences (no. 29Y127D01), the Fundamental Research Funds for the Central Universities (no. 861944), and the interdisciplinary Innovation Team of the Chinese Academy of Science.

Appendix A. Supplementary data

Supplementary data associated with this article can be found, in the online version, at http://dx.doi.org/10.1016/j.agrformet.2016.06.006.

References

Ali, M.F., Mawdsley, J.A., 1987. Comparison of two recent models for estimating actual evapotranspiration using only recorded data. J. Hydrol. 93, 257–276.
Allen, R.G., Pereira, L.S., Raes, D., Smith, M., 1998. Crop evapotranspiration. FAO Irrigation and Drainage Paper 56, 300 pp., Rome.
Anayah, F.M., Kaluarachchi, J.J., 2014. Improving the complementary methods to estimate evapotranspiration under diverse climatic and physical conditions. Hydrol. Earth Syst. Sci. 18, 2049–2064.
Bai, Y., Zhu, G.F., Su, Y.H., Zhang, K., Han, T., Ma, J.Z., Wang, W.Z., Ma, T., Feng, L.L., 2015. Hysteresis loops between canopy conductance of grapevines and meteorological variables in an oasis ecosystem. Agric. For. Meteorol. 319–327, 214–215.
Baldocchi, D.D., Xu, L.K., Kiang, N., 2004. How plant functional-type weather, seasonal drought, and soil physical properties alter water and energy fluxes of an oak-grass savanna and an annual grassland. Agric. For. Meteorol. 123, 13–39.
Bouchet, R.J., 1963. Évapotranspiration réelle et potentielle signification climatique. IASH Publ. 62, 134–142.
Brutsaert, W., Stricker, H., 1979. An advection-aridity approach to estimate actual regional evapotranspiration. Water Resour. Res. 15, 443–450.
Brutsaert, W., 1982. Evaporation Into the Atmosphere: Theory, History, and Applications. Springer, New York (299 pp).
Brutsaert, W., 2005. Hydrology, An Introduction. Cambridge Univ. Press, Cambridge (605 pp).
Businger, J.A., 1988. A note on the Businger-Dyer profiles. Boundary Layer Meteorol. 42, 142–151.
Carey, S.K., Barbour, S.L., Hendry, M.J., 2005. Evaporation from a waste-rock surface, key lake, saskatchewan. Can. Geotech. J. 42, 1189–1199.
Crago, R.D., Brutsaert, W., 1992. A comparison of several evaporation equations. Water Resour. Res. 28, 951–954.
Crago, R., Crowley, R., 2005. Complementary relationships for near-instantaneous evaporation. J. Hydrol. 300, 199–211.
Crago, R.D., Qualls, R.J., 2013. The value of intuitive concepts in evaporation research. Water Resour. Res. 49, 6100–6104.
Crago, R., Suleiman, A., 2005. Heat flux parameterization for sparse and dense grasslands with the analytical land atmosphere radiometer model (ALARM). Boundary Layer Meteorol. 114, 557–572.
Crago, R.D., Qualls, R.J., Feller, M., 2010. A calibrated advection-arid evaporation model requiring no humidity data. Water Resour. Res. 46, http://dx.doi.org/10.1029/2009WR008497 (W09519).
De Bruin, H.A.R., Hartogensis, O.K., Allen, R.G., Kramer, J.W.J.L., 2005. Regional advection perturbations in an irrigated desert (RAPID) experiment. Theor. Appl. Climatol. 80 (2), 143–152.
Deming, W.E., 1943. Statistical Adjustment of Data. John Wiley and Sons, Inc, New York.
Dingman, S.L., 2002. Physical Hydrology, 2nd ed. PrenticeHall, Upper Saddle River, N.J (646 pp.).
Domingo, F., Villagarcia, L., Brenner, A.J., Puigdefabregas, J., 1999. Evapotranspiration model for semi-arid shrub-lands tested against data from SE Spain. Agric. For. Meteorol. 95, 67–84.
Dyer, A.J., 1974. A review of flux-profile relationships. Boundary Layer Meteorol. 7, 363–372.
Evett, S.R., Kustas, W.P., Gowda, P.H., Anderson, M.A., Prueger, J.H., Howell, T.A., 2012. Overview of the bushland evapotranspiration and agricultural remote sensing experiment 2008 (bearex08): a field experiment evaluating methods for quantifying ET at multiple scales. Adv. Water Resour. 50, 4–19.
Falge, E., Baldocchi, D., Olson, R., Anthoni, P., Aubinet, M., Bernhofer, C., Burba, G., Ceulemans, R., Clement, R., Dolman, H., Granier, A., Gross, P., Grünwald, T., Hollinger, D., Jensen, N.-O., Katul, G., Keronen, P., Kowalski, A., Lai, C.T., Lawc, B.E., Meyers, T., Moncrieff, J., Moors, E., Munger, J.W., Pilegaard, K., Rannik, Ü., Rebmann, C., Suyker, A., Tenhunen, J., Tu, K., Verma, S., Vesala, T., Wilson, K., Wofsy, K., 2001. Gap filling strategies for defensible annual sums of net ecosystem exchange. Agric. For. Meteorol. 107, 43–69.
Fisher, J.B., Whittaker, R.J., Malhi, Y., 2011. ET come home: potential evapotranspiration in geographical ecology. Global Ecol. Biogeogr. 20, 1–18.
Foken, T., Mauder, M., Liebethal, C., Wimmer, F., Beyrich, F., Leps, J.P., Raasch, S., De Bruin, H.A.R., Meijninger, W.M.L., Bange, J., 2010. Energy balance closure for the LITFASS-2003 experiment. Theor. Appl. Climatol. 101, 149–160.
Foken, T., 2008. The energy balance closure problem: an overview. Ecol. Appl. 18 (6), 1351–1367.
Granger, R.J., Gray, D.M., 1989. Evaporation from natural nonsaturated surfaces. J. Hydrol. 111, 21–29.
Granger, R.J., 1989. A complementary relationship approach for evaporation from nonsaturated surfaces. J. Hydrol. 111, 31–38.
Han, S., Hu, H., Yang, D., 2011. A complementary relationship evaporation model referring to the Granger model and the advection-aridity model. Hydrol. Processes 24, 2094–2101.
Hobbins, M.T., Ramírez, J.A., Brown, T.C., 2001. The complementary relationship in estimation of regional evapotranspiration: an enhanced advection-aridity model. Water Resour. Res. 37, 1389–1403.
Hoffmann, W.A., Jackson, R.B., 2000. Vegetation–climate feedbacks in the conversion of tropical savanna to grassland. J. Clim. 13, 1593–1602.
Huntington, J.L., Szilagyi, J., Tyler, S.W., Pohll, G.M., 2011. Evaluating the complementary relationship for estimating evapotranspiration from arid shrublands. Water Resour. Res. 47, http://dx.doi.org/10.1029/2010WR009874 (W05533).
Jackson, R.B., Sperry, J.S., Dawson, T.E., 2000. Root water uptake and transport: using physiological processes in global predictions. Trends Plant Sci. 5 (11), 482–488.
Jung, M., Reichstein, M., Ciais, P., Seneviratne, S.I., Sheffield, J., Goulden, M.L., Bonan, G., Cescatti, A., Chen, J., de Jeu, R., Dolman, A.J., Eugster, W., Gerten, D., Gianelle1, D., Gobron, N., Heinke, J., Kimball, J., Law, B.E., Montagnani, L., Mu, Q., Mueller, B., Oleson, K., Papale, D., Richardson, A.D., Roupsard, O., Running, S., Tomelleri, E., Viovy, N., Weber, U., Williams, C., Wood, E., Zaehle, S., Zhang, K., 2010. Recent decline in the global land evapotranspiration trend due to limited moisture supply. Nature 467, 951–954.
Kahler, D.M., Brutsaert, W., 2006. Complementary relationship between daily evaporation in the environment and pan evaporation. Water Resour. Res. 42, http://dx.doi.org/10.1029/2005WR004541 (W05413).
Katul, G.G., Parlange, M.B., 1992. A Penman-Brutsaert model for wet surface evaporation. Water Resour. Res. 28, 127–132.
Kelliher, F.M., Leuning, R., Schulze, E.-D., 1993. Evaporation and canopy characteristics of coniferous forests and grasslands. Oeco 95, 153–163.
Lee, X., 1998. On micrometeorological observations of surfaceair exchange over tall vegetation. Agric. For. Meteorol. 91, 39–49.
Legates, D.R., McCabe, G.J., 1999. Evaluating the use of 'goodness-of-fit' measures in hydrologic and hydroclimatic model validation. Water Resour. Res. 35, 233–241.
Lhomme, J.-P., Chehbouni, A., 1999. Comments on dual-source vegetation-atmosphere transfer models. Agric. For. Meteorol. 94, 269–271.
Lhommea, J.P., Guilioni, L., 2006. Comments on some articles about the complementary relationship. J. Hydrol. 323, 1–3.
Li, X., Cheng, G., Liu, S., Xiao, Q., Ma, M., Jin, R., Che, T., Liu, Q., Wang, W., Qi, Y., Wen, J., Li, H., Zhu, G.F., Guo, J., Ran, Y., Wang, S., Zhu, Z., Zhou, J., Hu, X., Xu, Z., 2013. Heihe watershed allied telemetry experimental research (HiWATER): scientific objectives and experimental design. Bull. Am. Meteorol. Soc., http://dx.doi.org/10.1175/BAMS-D-12-00154.
Liu, S.M., Xu, Z.W., Wang, W.Z., Jia, Z.Z., Zhu, M.J., Bai, J., Wang, J.M., 2011. A comparison of eddy-covariance and large aperture scintillometer measurements with respect to the energy balance closure problem. Hydrol. Earth Syst. Sci. 15, 1291–1306.
Liu, S.M., Xu, Z.W., Zhu, Z.L., Jia, Z.Z., Zhu, M.J., 2013. Measurements of evapotranspiration from eddy-covariance systems and large aperture scintillometers in the Hai River Basin, China. J. Hydrol. 487, 24–38.
Liu, S.M., Xu, Z.W., Song, L.S., Zhao, Q.Y., Ge, Y., Xu, T.R., Ma, Y.F., Zhu, Z.L., Jia, Z.Z., Zhang, F., 2016. Upscaling evapotranspiration measurements from multi-site to the satellite pixel scale over heterogeneous land surfaces. Agric. For. Meteorol., http://dx.doi.org/10.1016/j.agrformet.2016.04.008.
Long, D., Singh, V.P., 2010. Integration of the GG model with SEBAL to produce time series of evapotranspiration of high spatial resolution at watershed scales. J. Geophys. Res. 115, http://dx.doi.org/10.1029/2010JD014092 (D21128).
Manzoni, S., Vico, G., Porporato, A., Katul, G., 2013. Biological constraints on water transport in the soil–plant–atmosphere system. Adv. Water Resour. 51, 292–304.
McDonald, A.J.S., Davies, W.J., 1996. Keeping in touch: responses of the whole plant to deficits in water and nitrogen supply. Adv. Bot. Res. 22, 229–300.

Monin, A.S., Obukhov, A.M., 1954. Basic laws of turbulent mixing in the ground layer of the atmosphere. Tr. Geofiz. Inst. Akad. Nauk SSSR 24, 163–187.
Monteith, J.L., 1965. Evaporation and environment. In: Proceedings of the 19th Symposium of the Society for Experimental Biology. Cambridge Univ. Press, New York, pp. 205–233.
Morton, F.I., 1983. Operational estimates of areal evapotranspiration and their significance to the science and practice of hydrology. J. Hydrol. 66, 1–76.
Nepstad, D.C., de Carvalho, C.R., Davidson, E.A., Jipp, P.H., Lefebvre, P.A., Negreiros, G.H., Dasilva, E.D., Stone, T.A., Trumbore, S.E., Vieira, S., 1994. The role of deep roots in the hydrological and carbon cycles of Amazonian forests and pastures. Nature 372, 666–669.
Oke, T.R., 1978. Boundary Layer Climates, 2nd edn. Mathuen, London.
Parlange, M.B., Katul, G.G., 1992. An advection-aridity evaporation model. Water Resour. Res. 28, 127–132.
Penman, H.L., 1948. Natural evaporation from open water bare soil and grass. Proc. R. Soc. Lond. Ser. A 193, 120–145.
Pettijohn, J.C., Salvucci, G.D., 2006. Impact of an unstressed canopy conductance on the Bouchet-Morton complementary relationship. Water Resour. Res. 42, http://dx.doi.org/10.1029/2005WR004385 (W09418).
Pettijohn, J.C., Salvucci, G.D., 2009. A new two-dimensional physical basis for the complementary relation between terrestrial and pan evaporation. J. Hydrometeorol. 10, 565–574.
Poblete-Echeverria, C., Ortega-Farias, S., 2009. Estimation of actual evapotranspiration for a drip-irrigated Merlot vineyard using a three-source model. Irrig. Sci. 28, 65–78.
Qualls, R.J., Gultekin, H., 1997. Influence of components of the advectionaridity approach on evapotranspiration estimation. J. Hydrol. 199, 3–12.
Salvucci, G.D., Gentine, P., 2013. Emergent relation between surface vapor conductance and relative humidity profiles yields evaporation rates from weather data. P. Natl. Acad. Sci. U. S. A. 110 (16), 6287–6291.
Seneviratne, S.I., Corti, T., Davin, E.L., Hirschi, M., Jaeger, E.B., Lehner, I., Orlowsky, B., Teuling, A.J., 2010. Investigating soil moisture–climate interactions in a changing climate: a review. Earth Sci. Rev. 99, 125–161.
Shuttleworth, J.W., Wallace, J.S., 1985. Evaporation from sparse crops and energy combination theory. Q. J. R. Meteorol. Soc. 111, 839–855.
Si, J.H., Feng, Q., Zhang, X.Y., Liu, W., Su, Y.H., Zhang, Y.W., 2005. 2005: Growing season evapotranspiration from *Tamarix ramosissima* stands under extreme arid conditions in northwest China. Environ. Geol. 48 (7), 861–870.
Szilagyi, J., Jozsa, J., 2009a. Analytical solution of the coupled 2-D turbulent heat and vapor transport equations and the complementary relationship of evaporation. J. Hydrol. 372, 61–67.
Szilagyi, J., Jozsa, J., 2009b. An evaporation estimation method based on the coupled 2-D turbulent heat and vapor transport equations. J. Geophys. Res. 114, http://dx.doi.org/10.1029/2008JD010772 (D06101).
Szilagyi, J., Hobbins, M., Jozsa, J., 2009. A modified advection-aridity model of evapotranspiration. J. Hydrol. Eng. 14 (6), 569–574.
Szilagyi, J., 2007. On the inherent asymmetric nature of the complementary relationship of evaporation. Geophys. Res. Lett. 34, http://dx.doi.org/10.1029/2006GL028708 (L02405).
Teuling, A.J., Seneviratne, S.I., Williams, C., Troch, P.A., 2006. Observed timescales of evapotranspiration response to soil moisture. Geophys. Res. Lett. 33, http://dx.doi.org/10.1029/2006GL028178 (L23403).
Teuling, A.J., Seneviratne, S.I., Stöckli, R., Reichstein, M., Moors, E., Ciais, P., Luyssaert, S., van den Hurk, B., Ammann, C., Bernhofer, C., Dellwik, E., Gianelle, D., Gielen, B., Grünwald, T., Klumpp, K., Montagnani, L., Moureaux, C., Sottocornola, M., Wohlfahrt, G., 2010. Contrasting response of European forest and grassland energy exchange to heatwaves. Nat. Geosci. 3, 722–727.
Tolk, J.A., Evett, S.R., Howell, T.A., 2006a. Advection influences on evapotranspiration of alfalfa in a semiarid climate. Agron. J. 98 (6), 1646–1654.
Tolk, J.A., Howell, T.A., Evett, S.R., 2006b. Nighttime evapotranspiration from alfalfa and cotton in a semiarid climate. Agron. J. 98 (3), 730–736.
Vesala, T., Launiainen, S., Kolari, P., Pumpanen, J., Sevanto, S., Hari, P., Nikinmaa, E., Kaski, P., Mannila, H., Ukkonen, E., Piao, S.L., Ciais, P., 2010. Autumn temperature and carbon balance of a boreal Scots pine forest in Southern Finland. Biogeosciences 7, 163–176.
Wang, K.C., Dickinson, R.E., 2012. A review of global terrestrial evapotranspiration: observation, modeling, climatology, and climatic variability. Rev. Geophys. 50, http://dx.doi.org/10.1029/2011RG000373 (RG2005).
Wang, J.M., Mitsuta, Y., 1992. Evaporation from the desert: some preliminary results of HEIFI. Boundary-Lay Meteorol. 59, 413–418.
Wang, G., Huang, J., Guo, W., Zuo, J., Wang, J., Bi, J., Huang, Z., Shi, J., 2010. Observation analysis of land-atmosphere interactions over the Loess Plateau of northwest China. J. Geophys. Res. 115, http://dx.doi.org/10.1029/2009JD013372 (D00K17).
Webb, E.K., Pearman, G.I., Leuning, R., 1980. Correction of the flux measurements for density effects due to heat and water vapour transfer. Quart. J. R. Meteorol. Soc. 106, 85–100.
Xu, C.-Y., Chen, D., 2005. Comparison of seven models for estimation of evapotranspiration and groundwater recharge using lysimeter measurement data in Germany. Hydrol. Processes 19, 3717–3734.
Xu, C.Y., Singh, V.P., 2005. Evaluation of three complementary relationship evapotranspiration models by water balance approach to estimate actual regional evapotranspiration in different climatic regions. J. Hydrol. 308, 105–121.
Xu, Z.W., Liu, S.M., Li, X., Shi, S.J., Wang, J.M., Zhu, Z.L., Xu, T.R., Wang, W.Z., Ma, M.G., 2014. Intercomparison of surface energy flux measurement systems used during the HiWATER-MUSOEXE. J. Geophys. Res. 118, 13140–13141.
Zhu, G.F., Su, Y.H., Li, X., Zhang, K., Li, C.B., 2013. Estimating actual evapotranspiration from an alpine grassland on Qinghai-Tibetan plateau using a two-source model and parameter uncertainty analysis by Bayesian approach. J. Hydrol. 476, 42–51.
Zhu, G.F., Li, X., Su, Y.H., Zhang, K., Bai, Y., Ma, J.Z., Li, C.B., Hu, X.L., He, J.H., 2014a. Simultaneous parameterization of the two-source evapotranspiration model by Bayesian approach: application to spring maize in an arid region of northwest China. Geosci. Model Dev. 7, 1467–1482.
Zhu, G.F., Su, Y.H., Li, X., Zhang, K., Li, C.B., Ning, N., 2014b. Modelling evapotranspiration in an alpine grassland ecosystem on Qinghai-Tibetan plateau. Hydrol. Processes 28 (3), 610–619.
Zhu, G.F., Lu, L., Su, Y.H., Wang, X.F., Cui, X., Ma, J.Z., He, J.H., Zhang, K., Li, C.B., 2014c. Energy flux partitioning and evapotranspiration in a sub-alpine spruce forest ecosystem. Hydrol. Processes 28 (19), 5093–5104.
de Rosnay, P., Polcher, J., 1998. Modelling root water uptake in a complex land surface scheme coupled to a GCM. Hydrol. Earth Syst. Sci. 2, 239–255.